GLIA 51:132–147 (2005)

Genetic Expression Profile of Olfactory Ensheathing Cells Is Distinct From That of Schwann Cells and Astrocytes

ADELE J. VINCENT,[1] JENNIFER M. TAYLOR,[2] DEREK L. CHOI-LUNDBERG,[1] ADRIAN K. WEST,[1] AND MENG INN CHUAH[1]*

[1]*NeuroRepair Group, School of Medicine, University of Tasmania, Tasmania, Australia*
[2]*Department of Statistics, Oxford Centre for Gene Function, University of Oxford, Oxford, United Kingdom*

KEY WORDS
microarray; real-time RT-PCR; cytokines; lysozyme; glia

ABSTRACT
Olfactory ensheathing cells (OECs) accompany the axons of olfactory receptor neurons, which regenerate throughout life, from the olfactory mucosa into the olfactory bulb. OECs have shown widely varying efficacy in repairing the injured nervous system. Analysis of the transcriptome of OECs will help in understanding their biology and will provide tools for investigating the mechanisms of their efficacy and interactions with host tissues in lesion models. In this study, we compared the transcriptional profile of cultured OECs with that of Schwann cells (SCs) and astrocytes (ACs), two glial cell types to which OECs have similarities. Two biological replicates of RNA from cultured OECs, SCs, and ACs were hybridized to long oligo rat 5K arrays against a common reference pool of RNA (50% cultured fibroblast RNA and 50% neonatal rat brain RNA). Transcriptional profiles were analyzed by hierarchical clustering, Principal Components Analysis, and the Venn diagram. The three glial cell types had similarly increased or decreased expression of numerous transcripts compared with the reference. However, OECs were distinguishable from both SCs and ACs by a modest number of transcripts, which were significantly enriched or depleted. Furthermore, OECs and SCs were more closely related to each other than to ACs. Expression of selected transcripts not previously characterized in OECs, such as Lyz, Timp2, Gro1 (Cxcl1), Ccl2 (MCP1), Ctgf, and Cebpb, was validated by real-time reverse transcription-polymerase chain reaction (RT-PCR); immunohistochemistry in cultured OECs, SCs, and ACs, and adult tissues was performed to demonstrate their expression at the protein level.

INTRODUCTION

Olfactory ensheathing cells (OECs) surround but do not myelinate the axons of olfactory receptor neurons (ORNs), which regenerate throughout life, from the peripheral nervous system (PNS) into the central nervous system (CNS). The ability of ORNs to extend axons in the mature CNS is likely due in large part to the presence of OECs. As a result, the use of OECs in experimental models of spinal cord injury (SCI) to promote repair has been attempted in several laboratories worldwide during the past decade. While some research groups have reported substantial axonal regeneration and functional recovery (Ramon-Cueto et al., 1998; Ramon-Cueto et al., 2000; Li et al., 2004), recent studies have expressed doubts as to the efficacy of these cells (Gomez et al., 2003; Ramer et al., 2004; Riddell et al., 2004). Schwann cells (SCs) also promote some regeneration in the CNS and are able to myelinate demyelinated CNS axons (Franklin, 2002). However, SCs and OECs behave differently when transplanted into CNS lesion sites, and also interact differently with astrocytes (ACs) in vitro, with OECs being better able to integrate with host tissues and ACs (Barnett and Riddell, 2004). Variability in OEC integration into CNS lesion sites may at least partially account for observed differences in efficacy (Li et al., 2004); however, the molecular mechanisms of cellular interactions between OECs and host tissues and ACs are not known.

The dearth of information regarding the molecular phenotype of OECs underpins the difficulty in resolving apparent conflicting empirical observations by different research groups experimenting with OEC transplants. This is complicated by the morphologically heterogeneous and plastic nature of OECs in culture (Van Den Pol and Santarelli, 2003; Vincent et al., 2003), which has made it difficult to define these cells comprehensively across different culture models and after transplantation in the nervous system. OECs share characteristics with both SCs and ACs, but are generally thought to resemble SCs more closely (Wewetzer et al., 2002; Barnett and Riddell, 2004). A deeper understanding of the genetic constitution of OECs is essential to facilitate manipulation of the interaction between OECs and surrounding tissues for the purpose of neural repair, and to better understand their place in the glial cell family. In this study, we have employed microarray technology to obtain a global genetic profile of OECs and have compared it with that of SCs and ACs. The qualitative and quantitative comparison of transcripts demonstrated many similarities amongst these three cell types,

Grant sponsor: International Institute for Research in Paraplegia; Grant sponsor: National Health and Medical Research Council.

*Correspondence to: .Meng Inn Chuah, Discipline of Anatomy and Physiology, Private Bag 24, University of Tasmania, Hobart, Tasmania, Australia 7001. E-mail:Inn.Chuah@utas.edu.au

Received 31 August 2004; Accepted 7 January 2005

DOI 10.1002/glia.20195

Published online 23 March 2005 in Wiley InterScience (www.interscience.wiley.com).

with OECs and SCs more closely related to each other than to ACs. Furthermore, OECs were distinguished from SCs and ACs by a small number of transcripts from a variety of gene families. Real-time RT-PCR has been performed to validate the microarray data, and immunostaining has been done to demonstrate the expression of the genes at the protein level.

MATERIALS AND METHODS

Cell Culture

All procedures conducted on animals were approved by the Animal Experimentation Ethics Committee of the University of Tasmania and are consistent with the Australian Code of Practice for the Care and Use of Animals for Scientific Purposes. The culture protocols were optimized to minimize the differences between the procedures, where possible. Tissues for cell culture were harvested from 2-day-old Hooded Wistar rats euthanized on ice. All cell types were cultured in DMEM + 10% fetal calf serum + 1% penicillin-streptomycin-amphotericin B solution (DMEM-10S; all products from Gibco-BRL, Carlsbad, CA), and grown directly on plastic in tissue culture flasks (TPP, Switzerland). The mitotic inhibitor cytosine-β-D-arabinofuranoside (AraC) was used as a common method for purification of OEC, SC, and AC cultures.

OECs were cultured as before (Chuah and Teague, 1999; Vincent et al., 2003) with further modifications. Briefly, olfactory nerve layer (ONL) and olfactory mucosa (OM) were pooled and digested in 0.25% trypsin (Gibco-BRL) + 0.03% collagenase (Sigma, St. Louis, MO) in MEM HEPES modification (MEMH; Sigma) for three 15-min incubations at 37°C. The tissue was triturated, filtered through nylon gauze with 80-μm pores, centrifuged for 10 min at 500*g* and plated in DMEM-10S in uncoated 25-cm^2 flasks. After 24 h, the culture was treated daily for 3 days with 100 μM AraC (Sigma) and expanded in 100 μg/ml bovine pituitary extract (BPE; Sigma) for 4 days. OECs were harvested at confluence after a total of 8 days in culture without passage.

Schwann cells were cultured as previously described (Brockes et al., 1979) with modifications. The brachial plexus and sciatic nerves were processed and cultured in uncoated 25-cm^2 flasks as for OECs, except that the AraC treatment was maintained for 4 days and the culture was expanded in 20 μg/ml BPE + 2 μM forskolin (Sigma) for 4 days. The confluent culture was passaged and reexpanded in 20 μg/ml BPE + 2 μM forskolin for 6–8 days. Schwann cells were harvested at confluence after a total of 14 days in culture. Passage was necessary in order to obtain a sufficient RNA yield for microarray analysis and did not affect culture purity.

Astrocytes were cultured as previously described (McCarthy and De Vellis, 1980) with modifications. Neocortical tissues were digested in 0.25% trypsin + 0.03% collagenase in MEMH for 30 min at 37°C and then processed as for OECs. After 9 days of growth in uncoated 75-cm^2 flasks, the confluent culture was shaken at 200 rpm for 18 h at 37°C in an orbital mixer incubator. Adherent cells were treated for 4 days with 20 μM AraC, rested for 24 h, passaged, and cultured for a further 7 days. Astrocytes were harvested at confluence after a total of 22 days in culture. Rat skin fibroblasts were cultured as previously described (Chuah et al., 2000) and were harvested at confluence after the third passage.

Fluorescence Immunocytochemistry for Culture Purity Check

Culture purity was checked by immunostaining as previously described (Vincent et al., 2003). Briefly, a small number of cells were replated onto coverslips when cultures were harvested, grown in DMEM-10S for 24 h and fixed in 4% paraformaldehyde. All antibodies were incubated for 1 h at room temperature and included monoclonal anti-p75^{NTR} (1:100; Clone 192, Chemicon, Temecula, CA), rabbit anti-glial fibrillary acidic protein (GFAP; 1:400; Dako Cytomation, Glostrup, Denmark), and AlexaFluor 488 goat anti-mouse IgG and AlexaFluor 594 goat anti-rabbit IgG (both 1:1,000; Molecular Probes, Eugene, OR). Cells were counterstained with Nuclear Yellow (0.0001%; Sigma).

RNA Sample Preparation and Experimental Design

Cultured cells were harvested at confluence with a rubber scraper and collected by centrifugation for 2 min at 500*g*. The resuspended pellet was homogenized in Buffer RLT (RNeasy Mini kit; Qiagen, Clifton Hill, Australia) by 10 passages through a 25-gauge needle and stored at −70°C. Whole brain excluding the olfactory bulbs was dissected from 2 day-old rats, snap-frozen in liquid N_2 and stored at −70°C. The tissue was homogenized in Buffer RLT, using an Ultra-Turrax T25 (IKA-Labortechnik, Staufen, Germany), followed by a QIAshredder Spin Column (Qiagen). Total RNA was extracted from cell cultures and brain tissue using the RNeasy Mini kit according to the manufacturer's instructions. RNA quality was confirmed by spectrophotometer analysis and gel electrophoresis.

Two pools of OEC, SC, and AC RNA were created from OEC, SC, and AC cultures, respectively. Each OEC RNA pool contained a total of six cultures, with each culture derived from three rats (18 rats total per pool). Each SC RNA pool contained 1.5 cultures, with each culture derived from nine rats (13.5 rats total per pool). In the case of the SCs, one of the cultures was used to supply RNA to both pools. Each AC RNA pool contained one culture derived from two rats. These RNA pools were hybridized to microarray chips against a common reference pool of RNA, which was composed of 50% cultured fibroblast RNA and 50% rat brain RNA. In addition, two internal control chips were made by the direct hybridization of OEC RNA against AC RNA.

Microarray Chips

Long (50mer) amino-modified oligonucleotides representing the Pan Rat 5K array (MWG-Biotech AG, Ebersberg, Germany) were printed in duplicate on Creative Chip Oligo Slides (Eppendorf-AG, Hamburg, Germany) at the Clive and Vera Ramaciotti Centre for Gene Function Analysis (UNSW, Sydney, Australia), using a ChipWriterPro microarray robot (Bio-Rad Laboratories, Hercules, CA) with Stelth Micro Spotting Pins (SMP3; Telechem International, Sunnyvale, CA). Immediately before hybridization, the microarray slides were baked at 65°C for 1 h, washed in 0.1% sodium dodecyl sulfate (SDS) at 95°C for 1 min, then in 5% ethanol at room temperature for 1 min, and dried immediately for 5 min at 800 rpm in an open 50-ml tube. The slides were not immersed in water at any stage.

RNA Labeling and Hybridization

Equal amounts of total RNA from each pool were hybridized to the microarrays. To make a red fluorescent probe, 15 μg of test RNA (OEC, SC, or AC) was labeled with Cyanine 5; to make green fluorescent probe, 15 μg of reference RNA was labeled with Cyanine 3. The probes were then competitively hybridized to a microarray chip. We used the amino–allyl–deoxynucleotide labeling method because this approach negates the need to perform dye swap experiments. The protocol was performed as follows.

In this study, 15 μg total RNA was incubated with 2 μg Primer P(DT)15 (Roche, Basel, Switzerland) and 40 U rRNasin (Promega, Annandale, Australia) for 10 min at 70°C. cDNA was synthesized using 600 U Superscript III (Invitrogen, Mount Waverley, Australia), 750 μM amino-allyl-dUTP (Sigma), 150 μM dTTP, and 500 μM dNTPs (Promega), 10 mM DTT, and 5× First Strand Buffer (Invitrogen) for 2.5 h at 50°C. The reaction was terminated at 95°C for 5 min; 20 mM EDTA and 40 mM NaOH were added, incubated at 65°C for 15 min, and then 40 mM HCl was added. The probe was purified on a Microcon-PCR Filter Unit (Millipore, North Ryde, Australia) as follows: 500 μl water was applied to the filter for 10 min at 1,000*g*; then 438 μl water + cDNA probe were applied for 16 min at 2,000*g*; 5 μl water was added and incubated 1 min; the filter was then inverted and the cDNA eluted for 2 min at 2,000*g*. Another 5 μl water was added and the elution repeated.

The probe was then conjugated to monofunctional NHS-ester Cyanine 3 or Cyanine 5 dye (Amersham Biosciences, Castle Hill, Australia) sufficient to label 3 nmol amino groups per reaction, for 1 h in 80 mM sodium bicarbonate, pH 9.0. Labeled probe pairs were combined and purified using a QIAquick PCR Purification kit (Qiagen) as follows: 35 mM sodium acetate, pH 5.2, and water was added to a total of 100 μl and then 500 μl PB Buffer was added; the mix was applied to the column for 30 s at 13,200 rpm; the flow-through was reloaded, centrifuged again, and washed 3 times with 750 μl 75% ethanol. The column was dried for 1 min at 13,200 rpm, incubated for 5 min in 100 μl EB Buffer; the cDNA was eluted by centrifugation as above. The elution procedure was repeated twice more. The efficiency of cDNA production and dye incorporation was determined by spectrophotometer analysis. The probe was ethanol-precipitated, resuspended in water, and added to 34 μl DIG Easy Hyb Solution (Roche), 40 μg Human COT-1 DNA (Invitrogen), and 40 μg polydA (Amersham Biosciences), and applied to a microarray slide in a hybridization chamber (GeneWorks, Hindmarsh, Australia) for 14–15 h at 37°C. The slide was washed twice in 1× SSC + 0.1% SDS for 10 min at 50°C, followed by 1× SSC and 0.1× SSC for 1–2 min each at room temperature, dried for 5 min at 800 rpm in a 50-ml tube, and immediately scanned in an Affymetrix/Genetic Microsystems 418 Array Scanner (Genetic Microsystems, Woburn, MA).

Microarray Analysis

Signal intensity data were acquired using GenePix Pro 3.0 (Axon Instruments, Union City, CA) and analyzed using GeneSpring 6 (Silicon Genetics, Redwood City, CA). The dataset was normalized by Lowess regression, and each chip was centralized to a ratio of 1.0. The dataset was filtered to reduce noise and saturated signal using a lower threshold of normalized signal intensity of 20 for reference and 0.5 for test and a common upper threshold of 45,000 in 100% of conditions (i.e., any transcripts with one or more missing datapoints or with any datapoint outside the signal intensity thresholds for noise were excluded from analysis). A total of 1841 transcripts was returned, which included 384 unknown and 1,400 unique and known. Statistical analysis of the data was performed by one-way analysis of variance (ANOVA) without multiple testing correction. A total of 445 transcripts had a significance level of $P \leq 0.05$, which included 97 unknown and 342 unique and known. Agglomeration hierarchical clustering was performed using the standard correlation metric with a separation ratio of 1.0 and a minimum branch distance of 0.001. GeneSpring was used to perform Principal Components Analysis (PCA) and construct Venn diagrams.

Real-Time RT-PCR

Except for the reference pool, RNA was extracted from cultures independent of those used in the microarray study. Reactions were performed in a Rotor-Gene 2000 cycler (Corbett Research, Mortlake, Australia) with appropriate controls, and each real-time run contained an amplicon standard curve. The QuantiTect SYBR Green RT-PCR kit (Qiagen) was used according to the manufacturer's instructions with 50 ng total RNA per sample and primers designed using Primer3 (Rozen and Skaletsky, 2000) and synthesized by Sigma. Primer pairs used were (forward and reverse, respectively): Ctgf CTGTGAGGAGTGGGTGTGTG and GTCAGGGCCAAATGTGTCTT (94-bp product); Unc5h2 GGAACCAGAGGATGCCTACA and CCACTCGCCATTACACTTGA (100-bp product); Timp2 GCATCACCCAGAAGAAGAGC and TGATGCAGGCAAAGAACTTG (174-bp product); Chl1 ATTTGTTGGGGAAAG-

CCAGT and AGATACCGTTGCTCCCTGTG (108-bp product); Lyz AGGAATGGGATGTCTGGCTA and TAGTCGGTGCTTTGGTCTCC (122-bp product); Ccl2 TGTTCACAGTTGCTGCCTGT and TGCTGCTGGTGATTCTCTTG (141-bp product); Gro1 CACACTCCAACAGAGCACCA and GTGAATCCCTGCCACTGTCT (148-bp product); GAPDH AAGTATGATGACATCAAGAAGGTGGT and AGCCCAGGATGCCCTTTAGT (67-bp product). Amplicon abundance was normalized to GAPDH abundance because this housekeeping gene was approximately equal across all microarray chips. Normalized amplicon levels were expressed as a ratio of the reference RNA to enable a direct comparison with the microarray data.

Immunostaining of Cultured OECs, ACs, and SCs, and Tissue Sections From Adult Rat

OECs, ACs, and SCs were cultured as above and replated at 2×10^4 cells on each 13-mm diameter coverslip. They were grown for 4 days in DMEM-10S and were fixed in 4% buffered paraformaldehyde before immunostaining.

Two adult Hooded Wistar rats were transcardially perfused under deep Nembutal anesthesia (50 mg/kg body weight) with cold phosphate-buffered saline (PBS) then cold 4% paraformaldehyde, pH 7.4. The rats were decapitated and the skin, eyes, and lower jaw were removed. The trimmed heads were postfixed overnight in 4% paraformaldehyde, pH 7.4, at 4°C. The specimens were washed in PBS for 6 h and decalcified in Fast-Cal Decalcifier (Histo-Labs, Riverstone, Australia) overnight at room temperature, then washed in tap water for 2 h and dehydrated in graded ethanol. Specimens were cleared overnight in chloroform, infiltrated with paraffin under vacuum and embedded in paraffin. Tissues were sectioned serially at 7 μm, and sections were placed on glass slides coated in 2% aminopropyltriethoxysilane (Sigma). Slides were dewaxed in xylene and hydrated through graded ethanol before immunostaining.

Endogenous peroxidase was quenched in 3% H_2O_2 for 5 min and nonspecific binding was blocked with DAKO Protein Block Serum-Free (Dako Cytomation) for 15 min. Primary antibodies were incubated for 1 h at room temperature for cultures and overnight at 4°C for tissue sections: goat anti-Ccl2 (also known as MCP1 and Scya2) (1:100, Santa Cruz Biotechnology), goat anti-Ctgf (1:100, Santa Cruz Biotechnology), rabbit anti-Cebpb (1:400, Santa Cruz Biotechnology), rabbit anti-Gro 1 (also known as Cxcl1) (1:100, Chemicon), rabbit anti-Timp2 (1:100, Promega), rabbit anti-human milk Lyz (1:200, Chemicon), rabbit anti-GFAP (1:400, Dako Cytomation), and mouse anti-βIII tubulin (1:5,000, Promega), goat anti-olfactory marker protein (OMP) (1:5,000, generous gift from Dr. Frank Margolis). Antibody labeling was visualized using the LSAB+ System-HRP kit and DAKO Liquid DAB+ Substrate-Chromogen System kit (Dako Cytomation) according to the manufacturer's instructions. Tissue was counterstained in Mayer's hematoxylin solution for 5 min, dehydrated through graded ethanols and xylene and mounted in DPX (Kock-Light Laboratories, Haverhill, UK). For negative controls the primary antibody was omitted.

RESULTS

Experimental Setup and Controls

In this microarray study, we used a common reference design, in which cell culture RNA pools from OECs, SCs, and ACs were normalized to a common "reference" RNA pool of 50% cultured fibroblast RNA and 50% neonatal rat brain RNA, with two biological replicate chips made for each. This enabled an indirect comparison among the three cell types. The morphology of OECs was mostly multipolar process-bearing, and phase-contrast images of OECs, SCs, and ACs in culture immediately before harvest are shown in Figure 1A–C. Immunofluorescence demonstrated that OEC cultures were 93% $p75^{NTR+}/GFAP^+$ cells, SC cultures were 98% $p75^{NTR+}$, and AC cultures were >98% $GFAP^+$ (Fig. 1D–F). It is possible that a small number of $p75^{NTR+}$ cells in OEC cultures were SCs. Other contaminating cell types in the OEC cultures were approximately 5% fibroblasts ($p75^{NTRV}/GFAP^V$) and 2% ACs ($GFAP^+$ only). Fibroblasts comprised the 2% of contaminating cells in SC cultures and the rare contaminating cells in AC cultures. While cellular contamination is an unavoidable limitation of using primary cultures for microarray analysis, we have taken significant steps to address this issue by adding fibroblast RNA to the reference pool in part to neutralize systematic variation from fibroblast contamination.

Self-selfhybridization of the reference RNA to the microarray (Pan Rat 5K array, MWG-Biotech AG) demonstrated expression of the vast majority of transcripts (data not shown). The 95% confidence intervals of the self-selfhybridizations corresponded to a fold-change range of 1.4–2.0, so we choose a fold-change threshold of $|>1.5|$ for analysis. Two internal control chips were made by direct hybridization of OEC and AC RNA and were consistent with the data from the common reference experiment (e.g., Table 1).

Glial Cell Relationships

We were interested in determining to what extent the transcriptome of OECs differed from that of SCs and ACs and whether we could identify specific genes that were highly expressed in OECs. Hierarchical clustering of the whole filtered dataset (1841 transcripts) generated a dendogram that separated the chips into three classes (Fig. 1G). Each class contained the replicate chips of one cell type. The second-order branching of the dendogram then classed OECs and SCs as more closely related to each other than to ACs (Fig. 1G). A similar result was obtained using the dataset of 445 significantly, differentially expressed transcripts (ANOVA $P \leq 0.05$; Fig. 1H), with the exception that replicates were more tightly clustered due to the filtering requirements of the one-

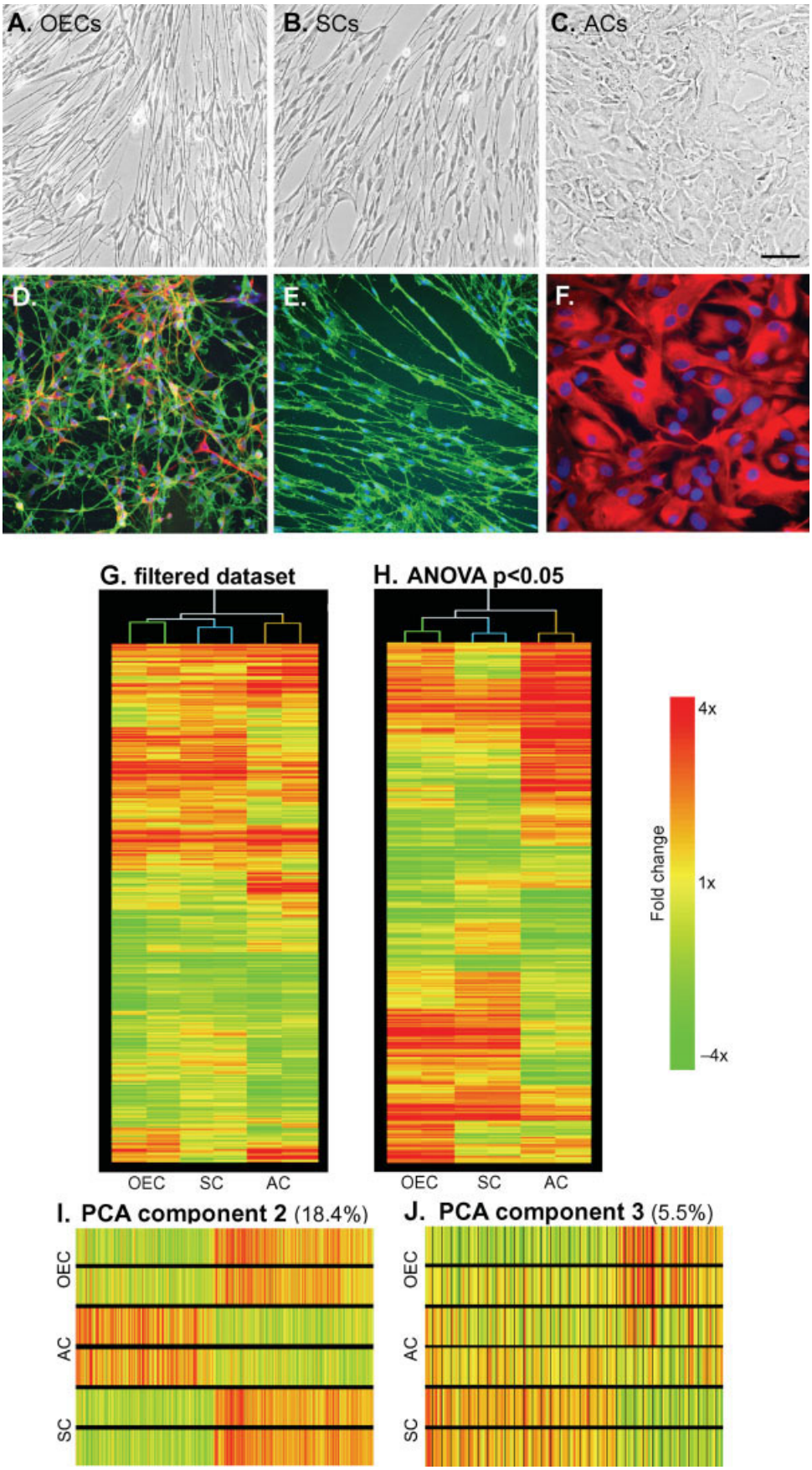

Fig. 1. Cell morphologies, hierarchical clustering and Principal Components Analysis of microarray data. **A–C:** Phase-contrast images of olfactory ensheathing cells (OECs, A), Schwann cells (SCs, B), and astrocytes (ACs, C) immediately before harvest for RNA extraction. **D–F:** Immunofluorescence of OECs (D), SCs (E), and ACs (F) replated at the time of RNA harvest and cultured for an additional 24 h. GFAP, red; p75NTR, green; nuclei, blue. **G,H:** Hierarchical clustering of the whole filtered microarray dataset (G) and significantly differentially expressed transcripts (H, ANOVA, $P < 0.05$). Each of the columns represents a chip (2 replicate chips per cell type), each row a transcript and transcripts are ordered by default gene trees generated in GeneSpring (not shown). **I,J:** Results of PCA analysis using the whole filtered dataset is shown for component 2 (I) and component 3 (J). The plots are ordered lists of transcripts with large +/− eigenvalues (0.6 to 1.0 and −0.6 to −1.0), where each row represents a chip and each column a transcript. Scale bar (G-J) is a colorimetric representation of the fold change of transcripts relative to reference. Scale bar = 10 μm in A (refers to A–C).

TABLE 1. Transcript Abundance of Common Glial Markers and Other Previously Described Genes

		Common reference chips[a]						Internal control chips[b]	
		OEC		AC		SC		OEC vs AC	
Genbank	Name	Replicate 1	Replicate 2	Replicate 1	Replicate 2	Replicate 1	Replicate 2	Replicate 1	Replicate 2
X01090	S-100β	1.02	2.49	10.13	3.45	−1.19	−1.36	−1.74	−2.44
X05137	$p75^{NTR}$	—[c]	14.19	—	1.13	—	—	15.81	—
AF028784	GFAP	—	—	43.58	24.46	1.56	—	−17.79	−15.34
M17784	PN-1	49.90	41.92	1.11	−1.66	23.65	16.53	52.33	38.65
J02582	apoE	1.64	1.53	5.59	5.44	−3.14	−2.53	−2.00	−1.91
K03242	P_0	3.87	3.80	−1.11	1.27	3.51	5.39	4.18	3.14

[a]Values are expressed as fold change relative to reference.
[b]Positive fold-change values indicate relative enrichment in OECs, negative values indicate relative enrichment in ACs.
[c]Transcripts with missing data points were filtered out in subsequent analyses.

way ANOVA test. Blocks of transcripts that are highly consistent within the replicate groups and differentially regulated across the three cell types can be clearly identified in Figure 1H.

Principal Components Analysis is a powerful, unsupervised method for reducing highly dimensional data to a number of components which describe the major sources of variation in the dataset. From PCA analysis of the whole filtered dataset, component 1 described 69.5% of the variance and included transcripts that were similarly enriched or depleted across all three cell types, relative to the reference (data not shown). The three cell types showed a high degree of relatedness, with most transcripts under common regulation. Component 2 described 18.4% of the variance and separated the data into two classes: ACs and OECs/SCs (Fig. 1I). An ordered list of transcripts with large ± eigenvalues for component 2 (Fig. 1I) shows that these transcripts have very similar expression profiles in OECs and SCs but have different profiles in ACs. Although 88% of the transcripts are commonly regulated in OECs and SCs, component 3 (5.5% of the variance, Fig. 1J) identified small sets of transcripts that were more abundant in OECs than in SCs (n = 48) and vice versa (n = 85).

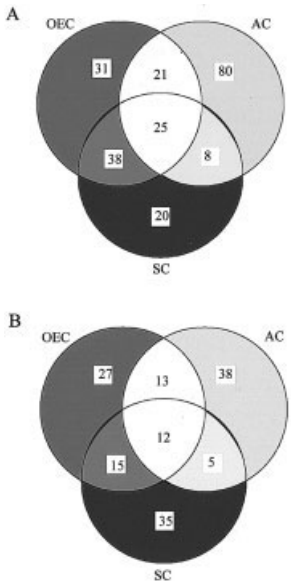

Fig. 2. Venn diagrams showing transcript distribution between the cell types. The diagrams were generated from lists of transcripts that are >1.5-fold **A** enriched and **B** depleted, relative to the reference, on a universe of differentially expressed transcripts (ANOVA, $P \leq 0.05$).

Transcriptional Profile of OECs

We next asked what is unique about the transcriptional profile of OECs. Venn diagrams were used to display the proportions of transcripts shared between the cell types. Two Venn diagrams were constructed from lists of transcripts that were greater than 1.5-fold enriched (Fig. 2A) or depleted (Fig. 2B) relative to the reference, on a universe of the ANOVA $P \leq 0.05$ dataset. Thus, the Venn diagrams contain only those transcripts which are up- or downregulated (by ± >1.5-fold) in at least one cell type and are also statistically differentially expressed across the cell types. These diagrams support the analysis described above, indicating that OECs and SCs are more closely related to each other than ACs, and also suggest that OECs may be slightly more related to ACs than SCs are.

Transcripts that are uniquely enriched (n = 18) or depleted (n = 22) in OECs were extracted using multiple Venn diagrams in order to maximize their robustness across replicates. These transcripts are listed according to the Rat Genome Database wherever possible in Table 2. The transcripts originate from a wide variety of gene families and no co-regulation of gene family members could be identified by gene ontology (not shown). Equivalent lists of transcripts for SCs and ACs are shown in Tables 3 and 4, respectively. The greater number of transcripts significantly enriched in ACs is consistent with its position as outlier relative to OECs and SCs.

Validation of the Microarray Data

Seven transcripts not previously characterized in OECs were chosen for validation by real-time RT-PCR and direct comparison with the microarray data (Fig. 3). For each transcript, amplicon abundance derived from RT-PCR was normalized to GAPDH abundance because this housekeeping gene was approximately equal across all microarray chips. The normalized amplicon levels were then expressed as a ratio of the reference RNA, hence the baseline value at the y-axis is 1. The x-axis indicates the three types of cells used in the experiment.

TABLE 2. OEC Transcripts Uniquely Enriched or Depleted

Genbank	Name	Fold[a]	*P*
D38629	Apc, adenomatosis polyposis coli	1.58	0.0268
X58294	Ca2, carbonic anhydrase 2	2.18	0.0034
M57235	Cebpb, CCAAT/enhancer binding protein (C/EBP), β	1.70	0.0194
AF069775	Chl1, cell adhesion molecule with homology to L1CAM (close homologue of L1)	2.57	0.0088
U95177	Dab2, disabled homologue 2, mitogen-responsive phosphoprotein (*Drosophila*)	1.72	0.0144
L00382	embryonic fibroblast tropomyosin 1[b]	3.19	0.0374
Y10889	Emp3, epithelial membrane protein 3	1.62	0.0045
M32062	Fcgr3, Fc receptor, lgG, low-affinity III	2.11	0.0220
L13206	Foxd4, forkhead box D4	2.00	0.0223
X07266	Gene 33 polypeptide[b]	2.78	0.0096
D11445	Gro1. gro	3.13	0.0121
AF001282	Hprt, hypoxanthine guanine phosphoribosyl transferase	1.70	0.0074
AF155822	Kif5b, kinesin family member 5B	2.44	0.0095
L12458	Lyz, lysozyme	6.57	0.0050
L12459	Lyz, lysozyme	3.39	0.0029
X79328	P5, protein disulfide isomerase-related protein	2.12	0.0138
U32438	Rgs11, regulator of G-protein signaling 11	1.99	0.0012
U87306	Unc5h2, transmembrane receptor Unc5H2	1.60	0.0032
AJ249986	Grf2, C3G protein	−1.90	0.0153
J04063	Camk2g, CaM kinase II γ	−1.78	0.0217
X95466	CPG2, CPG2 protein	−1.95	0.0429
AF131912	Efna2, ephrin A-2 precursor	−2.18	0.0016
X85184	Ragb, GTP-binding protein ragB	−3.04	0.0086
AF083328	Il12rb1, interleukin-12 receptor, β1	−1.54	0.0109
L35317	Idh1, isocitrate dehydrogenase 1	−2.46	0.0221
AF212861	Mir16, membrane interacting protein of RGS16	−1.58	0.0256
AB034800	Myh10, myosin heavy chain 10, nonmuscle	−2.35	0.0159
AB012234	Nfix, nuclear factor I/X	−1.85	0.0069
AF016252	Neb2, nuerabin 2	−2.07	0.0020
AB039878	Park2, parkin	−1.65	0.0353
X06890	Rab4a, member of RAS oncogene family	−1.94	0.0110
U25264	Sepw1, selenoprotein W, muscle 1	−1.75	0.0016
AB017638	Prss8, serine protease 8 (prostasin)	−1.91	0.0383
Y09179	TCR-α joining region, clone-library VA8s2F[b]	−1.96	0.0343
U89282	telomerase protein component[b]	−1.66	0.0296
AF112447	Tnxb, tenascin XB	−1.85	0.0150
AJ409332	Timp2, tissue inhibitor of metalloproteinase 2	−1.87	0.0002
AF335281	Tumor suppressor pHyde[b]	−1.58	0.0023
AF093623	Ucn, urocortin	−1.98	0.0391

[a]Average fold change of replicate chips.
[b]Not annotated according to the Rat Genome Database.

Four transcripts uniquely enriched in OECs, Chl1, Gro1 (Cxcl1), Lyz, and Unc5h2, and one transcript uniquely depleted in OECs, Timp2, were chosen from Table 2. In addition, Ccl2 (MCP1 or Scya2) and Ctgf which were non-significantly enriched 2-fold and 2.54-fold, respectively, in OECs were analyzed. In every case, the real-time RT-PCR results supported the microarray results (Fig. 3), with RT-PCR usually showing greater fold-differences in expression, consistent with the lower dynamic range of microarrays (Rajeevan et al., 2001).

Common markers of OECs such as $p75^{NTR}$ and S-100β displayed expected expression profiles, although in a few cases inadequately spotted probes meant that there were not sufficient replicates to analyze expression of these genes statistically (Table 1). Note that this issue affecting a small number of probes did not affect the analytical outcomes derived from Hierarchical clustering and PCA since transcripts which were not consistently detected across all replicates were filtered out before analysis. We have included other genes with previously described expression in one or more of the cell types as further validation of the microarray data: protease nexin-1 (PN-1), apolipoprotein E (apoE), and peripheral myelin protein P_0 (Table 1).

Characterization of Protein Expression in OECs, ACs, and SCs In Vitro

We then determined whether transcripts of interest were produced at the protein level in OECs, ACs, and SCs in order to gain some insight into the functional significance of the microarray data. We immunostained OECs, ACs and SCs in culture using a panel of antibodies, which included anti- Cebpb, Lyz, Ctgf, Timp2, Ccl2 (MCP1) and Gro1 (Cxcl1). Examples of the immunostaining are shown in Figure 4 and the relative staining intensities for each protein in OECs, ACs and SCs are presented in Table 5. Positive immunostaining for $p75^{NTR}$ was performed to ensure that cultured OECs and SCs were pure (Fig. 4A,C) while GFAP immunoreactivity was used to determine the purity of cultured ACs (Fig. 4B). Negative controls without primary antibodies had no reaction product (data not shown).

The relative protein expression levels were generally consistent with the upregulated level of transcripts in OECs. All proteins were detected in cultured OECs, albeit at very low levels for the chemokines Ccl2 (MCP1) and Gro1 (Cxcl1), which were detected primarily as punctate staining in the nucleus (Fig. 4P,S). Neverthe-

TABLE 3. Schwann Cell Transcripts Uniquely Enriched or Depleted

Genbank	Name	Fold[a]	*P*
U12402	Arl1, ADP-ribosylation factor-like 1	2.01	0.00749
AY008275	Casp9, caspase 9	2.17	0.02010
AF145445	Chga, chromogranin A	1.63	0.01630
X54080	Cox7a3, cytochrome c oxidase subunit 7a3	2.05	0.00213
X58631	Csk, protein-tyrosine kinase[b]	2.02	0.01790
AF321130	Hdac2, histone deacetylase 2	1.95	0.02200
AB016536	Hnrpab, heterogeneous nuclear ribonuclearprotein A/B	1.72	0.00826
U83897	Pscd3, pleckstrin homology, Sec7, and coiled/coil domains 3	2.19	0.00004
M60664	Ptma, prothymosin α	1.94	0.00950
L10415	Rabggta, Rab geranylgeranyl transferase a subunit	1.72	0.00442
X93352	Rpl10a, ribosomal protein L10a	1.76	0.04930
X62146	Rpl11, ribosomal protein L11[b]	1.66	0.01270
X07424	Rpl27, ribosomal protein L27	1.83	0.03730
M17422	Rpl7, ribosomal protein L7[b]	1.93	0.00255
AF009604	Sh3d2c1, SH3 domain protein 2 C1	2.12	0.01740
AJ004858	Sox11, Sry-box containing gene 11	2.84	0.00531
AF307852	Actr3, actin-related protein 3 homologue (yeast)	−1.72	0.04710
M77246	Ap2b1, adaptor-related protein complex 2, β 1 subunit	−1.54	0.04390
J02582	Apoe, apolipoprotein E	−2.80	0.00021
Y12635	Atp6b2, ATPase, lysosomal, β 56/58 kDa, isoform 2	−1.96	0.00987
D14441	Basp1, brain acidic membrane protein	−2.15	0.04600
M13095	brain 0-44, segment 2[b]	−1.57	0.00680
M97161	Caspg3, chondroitin sulfate proteoglycan 3	−2.14	0.00004
AF017437	Cd47, integrin-associated protein	−2.15	0.04060
AF314657	Clu, clusterin	−2.30	0.00578
D11339	Clu, clusterin	−1.57	0.00061
X16957	Cst3, cystatin C	−2.22	0.00027
S85184	Ctsl, cathepsin L proenzyme	−1.67	0.01220
U95177	Dab2, diabled homologue 2, mitogen-responsive phosphoprotein (*Drosophila*)	−2.01	0.01440
U48247	Enh, enigma homologue	−1.62	0.04280
X02610	Eno1, enolase 1, α	−1.99	0.00212
L29191	Fn1, fibronectin 1	−3.65	0.01620
AF106860	Gapd, glyceraldehyde-3-phosphate dehydrogenase	−1.58	0.00025
D42148	Gas6, growth arrest specific 6	−1.96	0.00268
M29599	Glns, glutamine synthetase 1	−2.64	0.00624
X61381	interferon-induced protein[b]	−3.11	0.04110
AF093773	Mdhl, malate dehydrogenase 1	−1.72	0.00805
D26179	Mtpn, myotrophin	−2.09	0.04650
D84346	Nckap1, NCK-associated protein 1	−2.13	0.01660
AF194442	Nrg1, neuregulin 1	−2.69	0.03780
AF086610	Odz2, odd Oz/ten-m homologue 2 (*Drosophila*)	−1.96	0.02100
AB041998	Ptges, prostaglandin E synthase	−1.99	0.02440
X56600	Sod2, superoxide dismutase 2	−2.39	0.04550

[a]Average fold change of replicate chips.
[b]Not annotated according to Rat Genome Database.

TABLE 4. Astrocyte Transcripts Uniquely Enriched or Depleted

Genbank	Name	Fold[a]	*P*
L14462	Aes, amino-terminal enhancer of split	1.72	0.00048
D13127	Atp5o, oligomycin sensitivity conferring protein	2.22	0.04650
X67215	Bsg, basigin	1.69	0.03080
Z46614	Cav, caveolin	2.21	0.00589
X76489	Cd9, CD9 antigen	5.57	0.00373
AF000578	Cdc5l, cell division cycle 5-like (*S. pombe*)	1.96	0.03790
M10140	Ckm, creatine kinase, muscle	2.12	0.02390
J04625	Cpe, carboxypeptidase E	2.28	0.00041
AF314540	Cryac, crystallin, α C	6.13	0.03420
M97161	Cspg3, chondroitin sulfate proteoglycan 3	4.13	0.00004
D17512	Csrp2, cysteine-rich protein 2	4.96	0.00052
X16957	Cst3, cystatin C	9.98	0.00027
AB009346	Dbnl, drebrin-like	1.93	0.03370
AF068861	Defb2, β defensin-2	3.48	0.00227
M60786	Ednra, endothelin receptor type A	2.55	0.02870
L14684	Efg, G elongation factor	1.72	0.03980
AB011532	Egfl3, MEGF6	1.97	0.03240
Y12502	F13a, coagulation factor XIIIa	1.77	0.04630
S69874	Fabp5, fatty acid binding protein 5, epidermal	1.67	0.00612
AF100960	Fat, FAT tumor suppressor homologue (*Drosophila*)	1.63	0.01520
M31591	Fst, follistatin	5.16	0.02480
X16145	Fuca, fucosidase αL-1, tissue	2.21	0.03520
AF255385	Gabre, γ-aminobutyric acid A receptor, ε	1.91	0.00287
D42148	Gas6, growth arrest specific 6	3.45	0.00268
M29599	Glns, glutamine synthetase 1	5.80	0.00624
X62660	glutathione transferase subunit 8[b]	2.80	0.03600
S61973	Grina, NMDA receptor glutamate-binding chain	3.68	0.01660

TABLE 4. (continued)

Genbank	Name	Fold[a]	*P*
M86389	heat shock protein 27[b]	14.97	0.00023
U95113	histone H2a gene[b]	1.59	0.00614
M33648	Hmgcs3, 3-hydroxy-3-methylglutaryl-Coenzyme A synthase 2	4.05	0.00319
J04486	lgfbp2, insulin-like growth factor binding protein 2	5.64	0.00119
L38644	Kpnb1, karyopherin, β 1	1.77	0.02520
AF242187	Lasp1, LIM, and SH3 protein 1	1.64	0.01030
U40001	Lipe, lipase, hormone-sensitive	2.18	0.00216
U40260	Lxn, latexin	4.18	0.02670
AF241614	Mcmd4, mini chromosome maintenance 4-deficient hormologue (*S. cerevisiae*)	3.20	0.02590
AF212861	Mir16, membrane interacting protein of RGS16	2.44	0.02560
S70011	mitochondrial tricarboxylate carrier[b]	2.52	0.02490
AB012234	Nfix. nuclear factor I/X	1.74	0.00692
U37058	Nmbr, neuromedin B receptor	3.04	0.02600
AF110508	Nos3, nitric oxide synthase 3, endothelial cell	1.57	0.01700
U58289	Nudt6, antisense basic fibroblast growth factor	1.82	0.00458
AJ243949	Pea15, phosphoprotein enriched in astrocytes, 15 kD[b]	9.27	0.00210
U10188	Plk, polo-like kinase homologue (*Drosophila*)	2.11	0.00961
X97375	Pnoc, prepronociceptin	2.22	0.01910
AF014009	Prdx6, peroxiredoxin 6	4.25	0.00107
M55601	Ptn, pleiotrophin	3.85	0.00744
AF254800	Rab0, GTP-binding protein Rab0	4.43	0.00672
AF051335	Rtn4, Nogo-A	3.07	0.03170
AJ132390	Sarip, small androgen receptor-interacting protein	2.92	0.01080
AB002151	Scarb1, scavenger receptor class B type I; SR-BI.	2.46	0.02670
M91808	Scn1b, sodium channel, voltage-gated, type 1, β polypeptide	3.92	0.00202
M81687	Sdc2, syndecan 2	2.04	0.00919
U25264	Sepw1, selenoprotein W, muscle 1	1.66	0.00157
M13979	Slc2a1, solute carrier family 2, member 1	2.55	0.01250
U59324	Slc3a2, solute carrier family 3, member 2	2.61	0.00582
X82021	St13, suppression of tumorigenicity 13, Hsp70-interacting protein	1.63	0.02620
M11566	Submaxillary gland S3 kallikrein[b]	2.78	0.00218
Y09185	TCR α variable region, clone-library DP10[b]	3.34	0.00601
D55648	Tcrg, T-cell receptor γ chain	8.21	0.00313
AJ409332	Timp2, tissue inhibitor of metalloproteinase 2	1.79	0.00017
X02411	Tpm1, tropomyosin 1, α	1.93	0.00595
S63830	Vamp3, vesicle-associated membrane protein 3	3.09	0.03680
M64780	Agm, agrin	−1.64	0.00132
U48288	Akap11, A kinase (PRKA) anchor protein 11	−1.76	0.02570
U72632	Aoc3, amine oxidase, copper containing 3	−2.22	0.02370
Y13380	Bin1, myc box-dependent interacting protein 1	−2.07	0.02880
L26268	Btg1, B cell translocation gene	−1.79	0.00042
Y10019	Cktsf1b1, cysteine knot superfamily 1, BMP antangonist 1	−3.46	0.00879
AF272662	Col5a1, collagen, type V, α 1	−5.56	0.00631
AJ224880	Col5a2, collagen, type V, α 2	−4.62	0.00168
AB023068	Ctgf, connective tissue growth factor	−3.20	0.00146
D00680	Gpx3, glutathione peroxidase 3	−3.64	0.03760
L05175	Gzmm, lymphocyte Met-ase 1	−2.36	0.00848
U55192	inpp5d, inositol polyphosphate-5-phosphatase D	−1.80	0.00261
AF071003	Kcne2, potassium voltage-gated channel, Isk-related family, member 2	−3.12	0.02860
AF087433	Lepre1, leprecan	−1.71	0.00111
X01785	Mox2, antigen identified by MRC OX-2	−2.44	0.02090
M86742	Ntf5, neurotrophin 5	−1.73	0.01380
AF086607	Odz2, odd Oz/ten-m homologue 2 (*Drosophila*)	−1.94	0.01650
X07320	Phkg1, phosphorylase kinase γ 1	−1.61	0.00272
M64092	Pkib, protein kinase (cAMP dependent, catalytic) inhibitor β	−3.72	0.01980
U52825	Sdc3, syndecan 3	−2.94	0.01320
AF260435	Sf3b1, splicing factor 3b, subunit 1, 155 LD	−1.60	0.03290
AF009604	Sh3d2c1, SH3 domain protein 2 C1	−2.00	0.01740
AJ004858	Sox11, SRY-box containing gene 11	−1.87	0.00531
AF140556	Tao2, serine/threonine protein kinase TAO2	−1.68	0.00024
U09401	Tnc, tenascin C	−2.73	0.00408
AB013732	Ugdh, UDP-glucose dehydrogenase	−2.74	0.00148
U87306	Unc5h2, transmembrane receptor Unc5H2	−1.98	0.00322
U78304	W307, W307 protein	−2.05	0.03850
AF329827	Zyx, zyxin	−1.71	0.00209

[a]Average fold change of replicate chips.
[b]Not annotated according to the Rat Genome Database.

less, the level of staining for Ccl2 and Gro1 in OECs could be observed clearly compared with that in ACs (Fig. 4Q,T) and SCs (Fig. 4R,U), which did not appear to express these two proteins. Immunohistochemical staining showed that transcripts that were downregulated in OECs in vitro did not necessarily translate to low levels of protein as shown by the high intensity of staining for Timp2 protein (Fig. 4M) compared with the very low level in ACs (Fig. 4N) and apparent lack of expression in SCs (Fig. 4O).

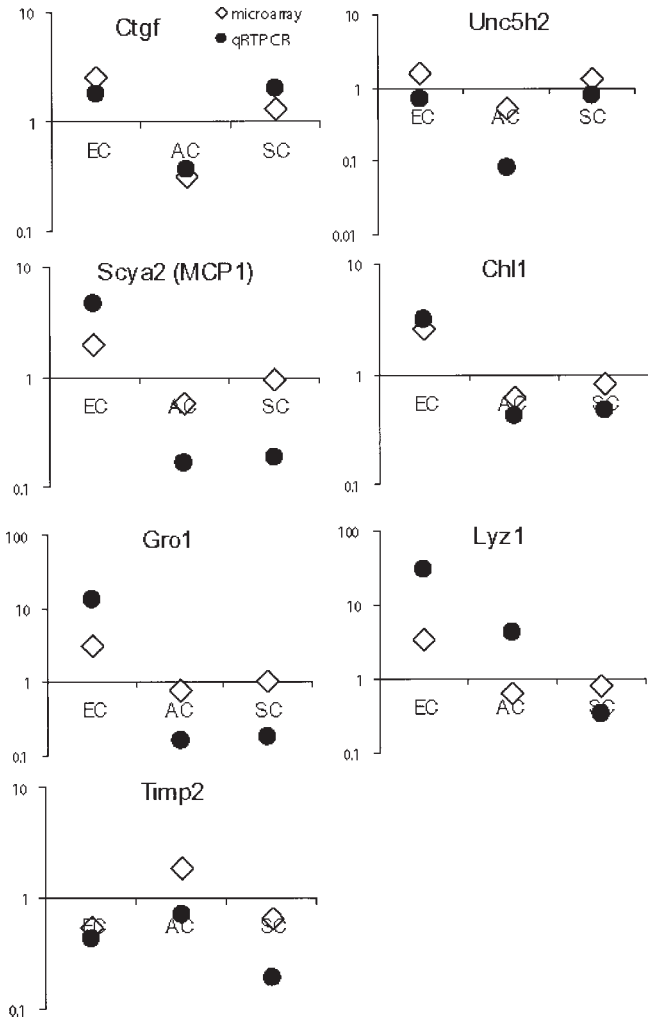

Fig. 3. Validation of microarray data by real-time RT-PCR. Differentially regulated transcripts validated by real-time RT-PCR were significant to $P \leq 0.05$ (except for Ccl2 [MCP1] and Ctgf). The microarray data from replicate chips were averaged to yield single datapoints for each cell type. The same reference RNA pool was used for both techniques but new test RNA was made for the real-time RT-PCR. For each transcript, amplicon abundance was normalized to GAPDH abundance because this housekeeping gene was approximately equal across all microarray chips. The normalized amplicon levels were then expressed as a ratio of the reference RNA. The y-axis defines the log expression relative to reference, with the baseline value set at 1. The x axis indicates the three types of cells used in the experiment.

Characterization of Protein Expression In Vivo

To gain further insight into the functional significance of the microarray data, we also determined whether transcripts of interest were produced at the protein level in the adult rat in vivo. Positive immunostaining for olfactory marker protein (OMP) was used to distinguish olfactory nerves from negatively staining trigeminal nerve fibers in the nasal cavity region (Fig. 5A). The astrocyte marker GFAP and neuronal marker βIII tubulin were used as standard references demonstrating expected staining patterns of astrocytes and axons, respectively. In the olfactory nerves and the olfactory nerve layer (ONL), Cebpb and Lyz were present in OECs, as were Ctgf and Timp2, to a lesser extent, with Timp2 only associated with a subpopulation of OEC nuclei (Fig. 5A,B, Table 5). Cebpb and Lyz appeared to be present also in olfactory axons and extensively in the olfactory bulb (Fig. 5B), suggesting that they may be present in the interneurons. Unlike OECs in vitro, OECs in vivo did not express detectable levels of Ccl2 (MCP1) and Gro1 (Cxcl1) (Fig. 5A,B). Gro1 (Cxcl1) appeared to label subpopulations of mitral and tufted cells and their processes in the olfactory bulb (Fig. 5B). Schwann cells of the trigeminal nerve expressed all the proteins present in OECs, and in the case of Cebpb at a relatively higher level (Fig. 5A). Interestingly, there was variability, for example, in the relative protein levels of Cebpb, Lyz, and Ctgf between Schwann cells in trigeminal nerves in olfactory mucosa and those present in peripheral nerves associated with the lacrimal gland (insets in Fig. 5A).

Except for Ctgf, which was localized to a subpopulation of nuclei, astrocytes in the cerebral cortex did not demonstrate expression of Cebpb, Lyz, Timp2, Ccl2 (MCP1), and Gro1 (Cxcl1) at the protein level (Table 5, Fig. 5C). Interestingly, in areas where the accessory olfactory bulb was closely apposed to the frontal cortex, the vomeronasal nerve layer was observed to express Lyz and Gro1 (Cxcl1) (Fig. 5C).

DISCUSSION

To our knowledge, this study is the first gene profiling conducted on cultured OECs by microarray analysis. We have shown that although OECs, SCs, and ACs share many transcriptional similarities, OECs and SCs are more closely related to each other than ACs; furthermore, OECs can be distinguished from SCs and ACs by their differential expression of certain transcripts. Several transcripts that have not been characterized previously in OECs were shown to be expressed at the protein level in cultured OECs and most of them in the adult olfactory system by immunohistochemistry.

Immunohistochemistry provides additional information regarding the expression of genes at the protein level and their possible functional effects. Because there are additional factors influencing the translation of RNA into proteins, protein levels and RNA do not necessarily correlate in every case as shown by data relating to Timp2 (see Figs. 3 and 4A).

The characterization of OECs in this study as being very similar to SCs and ACs, but more closely related to SCs than to ACs, is consistent with previous reports. For example, the expression of connexin family members, which form gap junctions between cells, and dye coupling behavior in vitro is similar but not identical among OECs, SCs, and ACs, with OECs and SCs being more similar (Barnett et al., 2001). OECs in vitro can adopt morphologies similar to ACs or SCs (Barnett and Riddell, 2004), and in fact can switch between the two (Vincent et al., 2003). While OECs and ACs share some

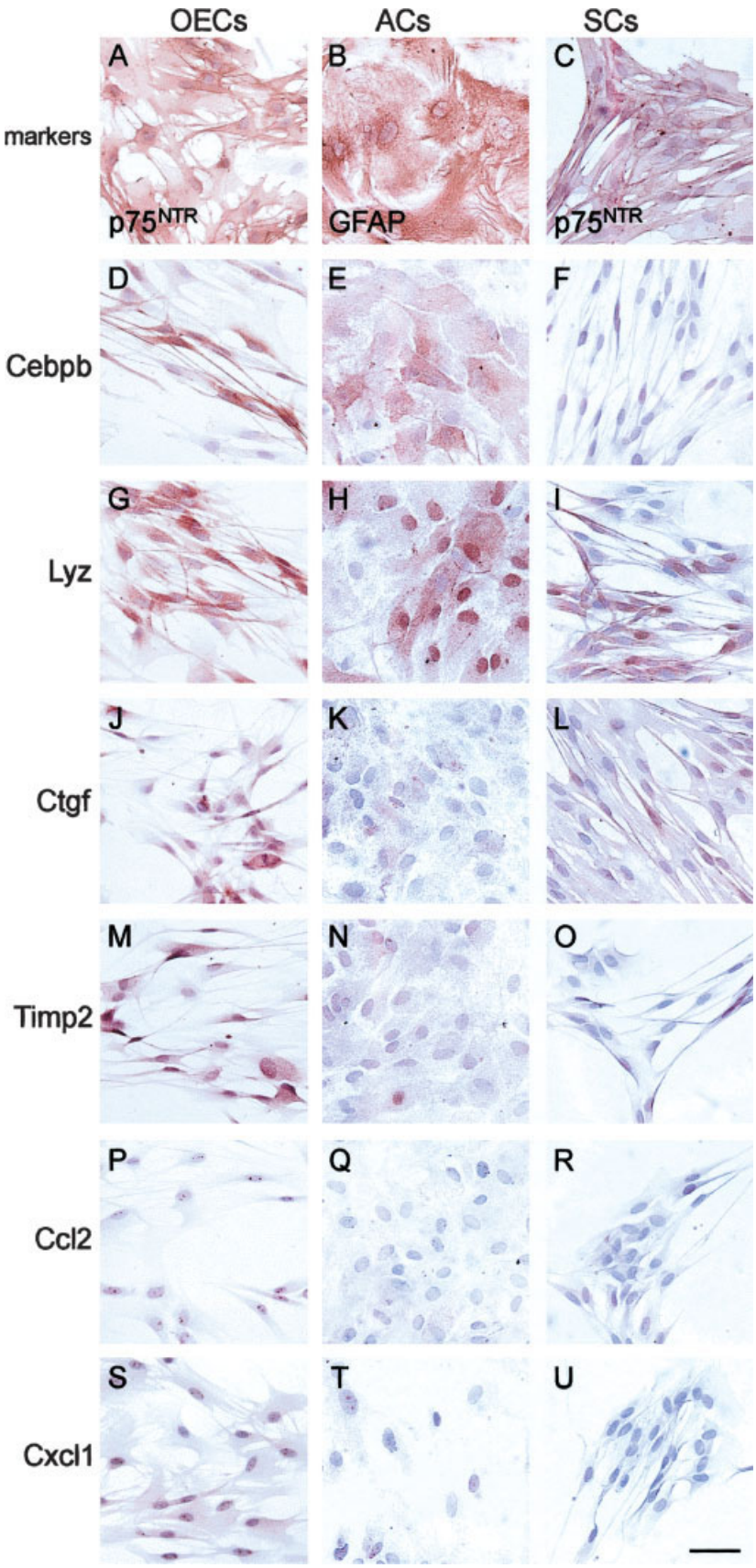

Fig. 4. Immunostaining of olfactory ensheathing cells, astrocytes and Schwann cells in vitro. Olfactory ensheathing cells (OECs, **A,D,G,J,M,P,S**), astrocytes (ACs, **B,E,H,K,N,Q,T**) and Schwann cells (SCs, **C,F,I,L,O,R,U**) in culture were stained using a panel of antibodies against the gene products of selected transcripts detected by microarray analysis: Cebpb (**D–F**), Lyz (**G–I**), Ctgf (**J–L**), Timp2 (**M–O**), Ccl2 (MCP1, **P–R**), and Cxcl1 (Gro1, **S–U**). Purity of OECs and SCs was determined by immunostaining for $p75^{NTR}$ (A and C, respectively) while glial fibrillary acidic protein (GFAP) was used as a marker for ACs (B). Immunostaining appears red/brown, and all cultures were counterstained with hematoxylin (purple). Olfactory ensheathing cells showed positive immunoreactivity for Cebpb (D), Lyz (G), Ctgf (J), Timp2 (M) and, to a lesser extent, Ccl2 (P) and Cxcl1 (S). ACs were positive for Cebpb (E), Lyz (H), and to a lesser extent Timp2 (N). SC were positive for Lyz (I) and, to a lesser extent, Ctgf (L). Scale bar = 50 μm.

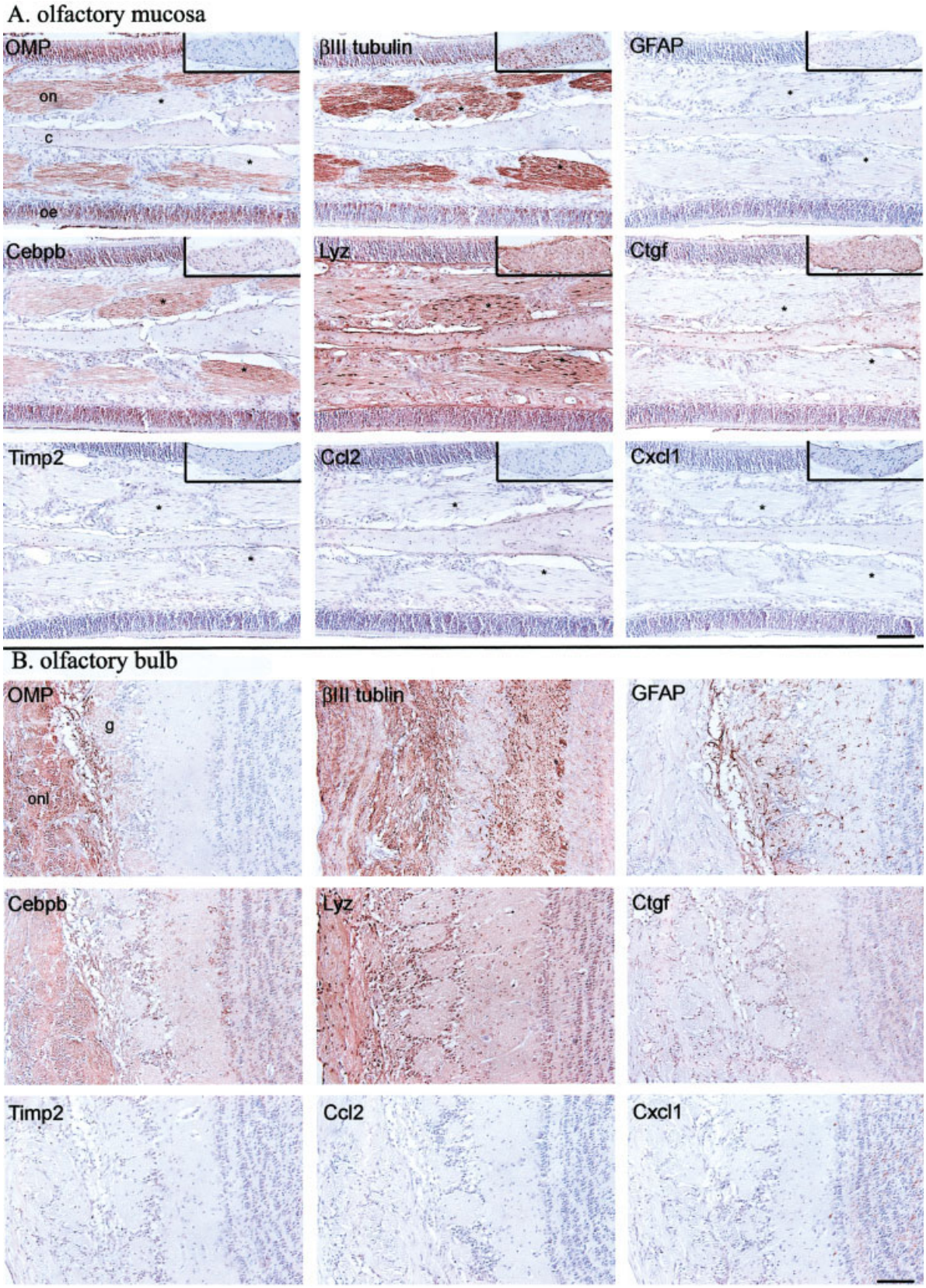
A. olfactory mucosa
OMP
on
c
oe
βIII tubulin
GFAP
Cebpb
Lyz
Ctgf
Timp2
Ccl2
Cxcl1
B. olfactory bulb
OMP
g
onl
βIII tublin
GFAP
Cebpb
Lyz
Ctgf
Timp2
Ccl2
Cxcl1

Figure 5.

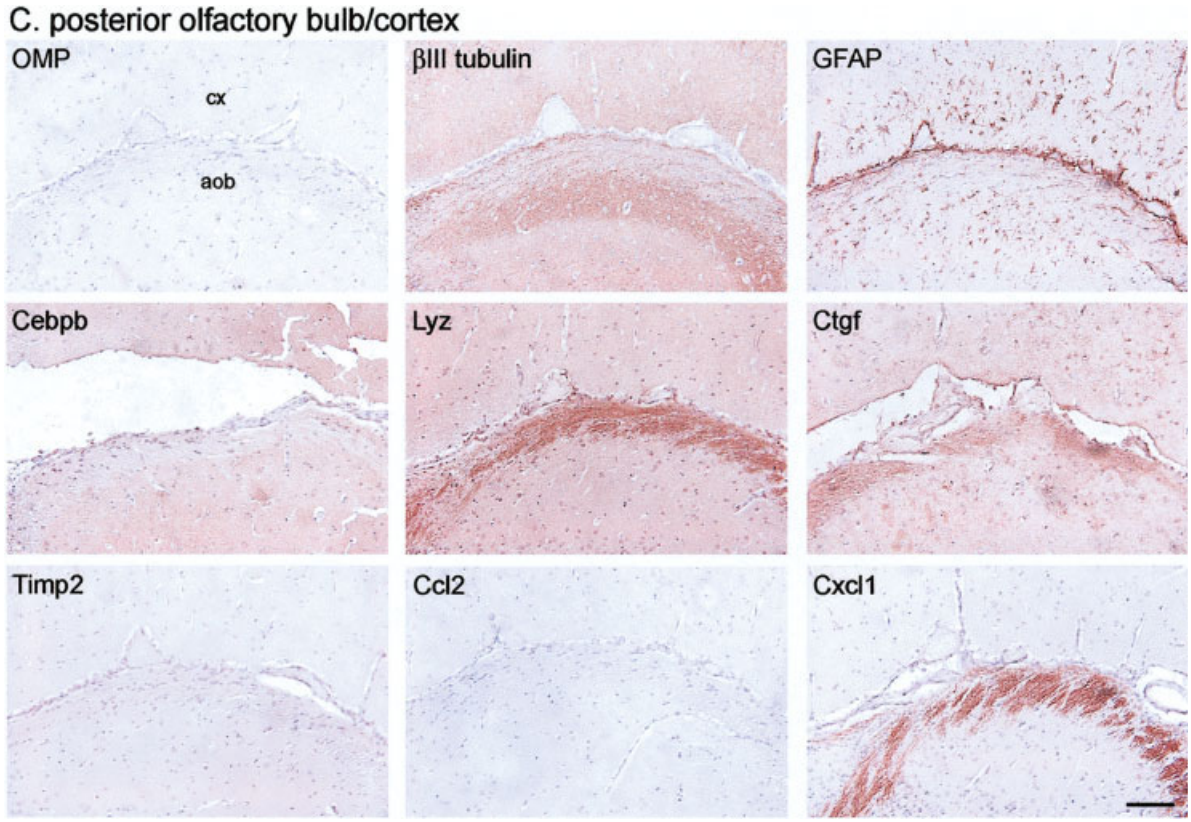

Fig. 5. Immunostaining of olfactory mucosa, olfactory bulb and cerebral cortex of adult rat. Immunohistochemistry (red/brown reaction product) was performed on tissue sections from olfactory mucosa (**A**), olfactory bulb (**B**), and posterior olfactory bulb/cortex (**C**), using antibodies against olfactory marker protein (OMP), βIII tubulin, glial fibrillary acidic protein (GFAP), Cebpb, Lyz, Ctgf, Timp2, Ccl2 (MCP1), and Cxcl1 (Gro1). Sections were counterstained with hematoxylin (purple). Positive immunostaining for OMP was used to distinguish the olfactory nerves (on) from the negatively stained trigeminal nerve fibers (asterisks, Fig. 5A) in the olfactory mucosa (**A**) on either side of the cartilaginous nasal septum (c), beneath the olfactory epithelium (oe). The OMP-positive nerves extend to the olfactory nerve layer (onl), which is peripheral to the glomerular layer (g) of the bulb (**B**). The posterior region of the olfactory bulb contains the accessory olfactory bulb (aob), which is closely apposed to the frontal cortex (cx) (**C**). GFAP and βIII tubulin were used as standard references demonstrating expected staining patterns of astrocytes and axons, respectively. Insets in A show the immunostaining pattern of a peripheral nerve associated with the lacrimal gland. Although proteins expressed by OECs in the olfactory mucosa (A) were also present in SCs in the trigeminal (asterisks) and other peripheral nerves (insets in A) the relative levels of the proteins varied in the case of Cebpb, Lyz, and Ctgf. Cebpb and Lyz also appeared to be present in axons and in extensive parts of the olfactory bulb, possibly including interneurons. Posteriorly, the vomeronasal nerve layer of the accessory olfactory bulb (aob) showed positive staining for Lyz and Cxcl1 (Gro1) and, to a lesser extent, Ctgf (C). Scale bar = 100 μm.

antigenic properties, such as expression of PSA-NCAM and GFAP (Franceschini and Barnett, 1996), OECs share with SCs an antigenic profile so similar as to prevent the cell types from being readily distinguished in culture or in OEC-implanted lesions (Barnett and Riddell, 2004; Wewetzer et al., 2002). While OECs and ACs share some functional characteristics, such as the ability to form the glial limitans of the olfactory bulb (Doucette, 1990), OECs and SCs share the ability to repair injured peripheral (Ramon-Cueto and Nieto-Sampedro, 1994; Navarro et al., 1999) and central nervous tissue (Li et al., 1997; Ramon-Cueto et al., 1998; Imaizumi et al., 2000; Lu et al., 2001), and to form peripheral-type myelin (Franklin et al., 1996; Imaizumi et al., 1998; Kato et al., 2000; Radtke et al., 2004).

However, at least three substantial differences exist between OECs and SCs. First, they interact differently with ACs in culture (Lakatos et al., 2000) and in the lesioned CNS environment (Lakatos et al., 2003; Garcia-Alias et al., 2004). Second, the regulation of myelin formation by the two cell types differs (Devon and Doucette, 1995), with OECs expressing the myelin-regulating transcription factor Krox-20 (like SCs) but little SCIP (unlike SCs) when transplanted into the demyelinated spinal cord (Smith et al., 2001). Third, OECs and SCs are developmentally distinct, being olfactory placode- and neural crest-derived, respectively. These differences are consistent with our finding that OECs and SCs are transcriptionally distinct. This distinction is apparent under similar conditions in culture, with even greater differences revealed by a comparison of the immunohistochemical staining of OECs and SCs in vivo.

The presence of transcripts and their products not previously characterized in OECs points to future lines of investigation into possible unsuspected biological roles for OECs. For example, OECs may have antimicrobial functions in the olfactory system, which may also contribute to their efficacy in repairing injured CNS tissue.

TABLE 5. Protein Expression in OECs, ACs, and SCs

	In vitro			In vivo		
Protein	OECs	ACs	SCs	OECs	ACs	SCs
Cebpb	+++	++	−	++	−	+++/+[a]
Lyz	+++	++	++	+++	−	+++/++
Ctgf	++	−	+	+	+[b]	+/++
Timp2	++	+	−	+[b]	−	+/−[b]
Ccl2	+	−	−	−	−	−/−
Cxcl1	+	−	−	−	−	−/−

[a]Trigeminal nerve in nasal cavity/peripheral nerve in lacrimal gland.
[b]Present in a subpopulation of nuclei.

Notably, OECs show increased abundance of two separate transcripts of the lysozyme gene (6.57- and 3.39-fold change, Table 2) as well as robust protein expression in culture and in the olfactory system (Table 5). A role for lysozyme activity in OECs is consistent with the susceptibility of the primary olfactory pathway to external chemical and pathogenic insults. A recent study showed that pneumococcal infection can occur from the olfactory epithelium to the olfactory bulb via transport along olfactory nerves, but that this route is limited by an unknown mechanism (van Ginkel et al., 2003).

Likewise, factors involved in the immune response and inflammation have been detected as transcripts enriched in OECs, including the chemokines Gro1 (Cxcl1, 3.13-fold, Table 2) and MCP1 (Ccl2, 2-fold). The protein levels for these factors are low or undetectable in OECs in vitro and in normal olfactory tissue (Table 5, Figs. 4P,S, 5A,B), but this is consistent with the expression of Ccl2 (MCP1) in SCs, which is normally low in the sciatic nerve and is upregulated in response to injury (Toews et al., 1998). Similarly, activated ACs produce a number of chemokines including Ccl2 (MCP1) in response to traumatic injury (Babcock et al., 2003) and demyelination in multiple sclerosis (Van Der Voorn et al., 1999). Gro1 (Cxcl1) is a neutrophil chemoattractant that is also involved in glial development. Astrocytes in the spinal cord produce Gro1 (Cxcl1) in a spatiotemporal manner to help direct oligodendrocyte precursor maturation and migration (Tran and Miller, 2003). Although OECs do not appear to produce Ccl2 (MCP1) or Gro1 (Cxcl1) in normal adult olfactory tissue (Table 5), a role for these factors may exist in OECs during embryogenesis or when these cells are transplanted into the injury site.

Furthermore, it is likely that OECs are themselves capable of responding to immune factors, as suggested by the enrichment of transcripts for the interleukin 6 (IL-6)-responsive transcription factor, Cebpb (1.70-fold, Table 2), and the constitutive production of its protein in OECs (Table 5, Fig. 4D). This notion is supported by a study that reported that in the aftermath of bulbectomy and following infiltration of IL-6 producing macrophages into the olfactory lamina propria, OECs were shown to upregulate their expression of IL-6 receptors (Nan et al., 2001). The authors of the study proposed that IL-6 may be involved in initiating intracellular signalling processes that ultimately lead to OECs establishing extracellular matrices which facilitate olfactory axonal regrowth (Nan et al., 2001). Such a capability could be functionally significant as well when OECs are transplanted into an acute injury site.

This study has revealed genes such as Chl1, Ctgf and Timp2 whose role in OEC-mediated repair warrants further investigation, especially in the context of glial scarring (Lakatos et al., 2003; Garcia-Alias et al., 2004) and neoangiogenesis (Richter et al., 2003). Ctgf is involved in diverse processes in the nervous system, which include angiogenesis, fibrotic and glial scarring, and extracellular matrix remodeling in normal and injured tissue (Hertel et al., 2000; Schwab et al., 2001). Timp2 is also involved in tissue remodeling as the inhibitory part of a matrix metalloproteinase complex. It is produced by both ACs (Muir et al., 2002) and SCs (Huang et al., 2000) and is thought to be involved in the suppression of neoangiogenesis by SCs. In the olfactory system, Ctgf has been observed in the embryonic mouse olfactory epithelium (Surveyor and Brigstock, 1999) and Timp2 expression is induced during regeneration in the injured adult mouse olfactory epithelium (Tsukatani et al., 2003).

A recent study has reported that gene expression was differentially altered in the acute leukemia cell line CCRF-CEM and the chronic myelogenous leukemia cell line K562 treated with AraC (Takagaki et al., 2003). Although we use AraC as part of the purification protocol for OECs, we have noted that fibroblasts were most sensitive to AraC, which induced the cells to undergo apoptosis, thus increasing the proportion of OECs in culture. We cannot completely discount the possibility that a few OECs may be selected out by this procedure but we are certain that the large majority of OECs remain viable and express growth-promoting properties as shown by their expression of growth factors in vitro (Woodhall et al., 2001) and their ability to promote repair in the injured spinal cord (Chuah et al., 2004)

Although this study is limited by the absence of expressed sequence tags in the microarrays we used, we have now generated a list of transcripts that are enriched in OECs compared with SCs and ACs in culture (Table 2). These could be investigated further to determine whether any of them are upregulated in OECs under a variety of conditions, i.e., in vitro, in vivo, or transplanted to a novel environment such as a lesion site in the CNS. The availability of additional markers for OECs would be useful, given that transplantation studies utilizing $p75^{NTR}$ immunostaining are unable to distinguish transplanted OECs from invading SCs which also express $p75^{NTR}$ (Takami et al., 2002). This could prove to be a challenging task due to the fundamentally different and novel environment of CNS lesions, and to the morphologically and antigenically plastic nature of OECs in vitro and in vivo (Pixley, 1992; Franceschini and Barnett, 1996; Vincent et al., 2003). For example, neuregulin expression in OECs is changed markedly by transplantation into the spinal cord, suggesting that the extrinsic environment exerts a profound effect on OEC phenotype (Woodhall et al., 2003). Nevertheless, a micro-

array study may now be initiated to investigate the in vivo phenotypes of OECs by laser capture or of encapsulated OECs which had previously been transplanted into a lesion site in the CNS (Chuah et al., 2004; Woodhall et al., 2003). In addition to identifying new markers for OECs, such studies will extend our understanding of OEC biology, which is essential in future experimentation to achieve a favorable outcome in CNS repair.

ACKNOWLEDGMENTS

The authors thank Dr. Nick Hayward for the use of his laboratory for hybridization and analysis at the Queensland Institute of Medical Research (Brisbane, Australia). We also thank Dr. Sandra Pavey for supplying the hybridization protocol as well as Dr. Nick Hayward and Nick Matigian for valuable assistance with experimental design and troubleshooting. We thank Kate Brettingham-Moore for the gift of GAPDH primers and all members of the NeuroRepair Group for their support of this work.

REFERENCES

Babcock AA, Kuziel WA, Rivest S, Owens T. 2003. Chemokine expression by glial cells directs leukocytes to sites of axonal injury in the CNS. J Neurosci 23:7922–7930.

Barnett SC, Riddell JS. 2004. Olfactory ensheathing cells (OECs) and the treatment of CNS injury: advantages and possible caveats. J Anat 204:57–67.

Barnett SC, Thompson RJ, Lakatos A, Pitts J. 2001. Gap junctional communication and connexin expression in cultured olfactory ensheathing cells. J Neurosci Res 65:520–528.

Brockes JP, Fields KL, Raff MC. 1979. Studies on cultured rat Schwann cells. I. Establishment of purified populations from cultures of peripheral nerve. Brain Res 165:105–118.

Chuah MI, Teague R. 1999. Basic fibroblast growth factor in the primary olfactory pathway: mitogenic effect on ensheathing cells. Neuroscience 88:1043–1050.

Chuah MI, Cossins J, Woodhall E, Tennent R, Nash G, West AK. 2000. Glial growth factor 2 induces proliferation and structural changes in ensheathing cells. Brain Res 857:265–274.

Chuah MI, Choi-Lundberg D, Weston S, Vincent AJ, Chung RS, Vickers JC, West AK. 2004. Olfactory ensheathing cells promote collateral axonal branching in the injured adult rat spinal cord. Exp Neurol 185:15–25.

Devon R, Doucette R. 1995. Olfactory ensheathing cells do not require L-ascorbic acid in vitro to assemble a basal lamina or to myelinate dorsal root ganglion neurites. Brain Res 688:223–229.

Doucette R. 1990. Glial influences on axonal growth in the primary olfactory system. Glia 3:433–449.

Franceschini IA, Barnett SC. 1996. Low-affinity NGF-receptor and E-N-CAM expression define two types of olfactory nerve ensheathing cells that share a common lineage. Dev Biol 173:327–343.

Franklin RJ. 2002. Remyelination of the demyelinated CNS: the case for and against transplantation of central, peripheral and olfactory glia. Brain Res Bull 57:827–832.

Franklin RJ, Gilson JM, Franceschini IA, Barnett SC. 1996. Schwann cell-like myelination following transplantation of an olfactory bulb-ensheathing cell line into areas of demyelination in the adult CNS. Glia 17:217–224.

Garcia-Alias G, Lopez-Vales R, Fores J, Navarro X, Verdu E. 2004. Acute transplantation of olfactory ensheathing cells or Schwann cells promotes recovery after spinal cord injury in the rat. J Neurosci Res 75:632–641.

Gomez VM, Averill S, King V, Yang Q, Perez ED, Chacon SC, Ward R, Nieto-Sampedro M, Priestley J, Taylor J. 2003. Transplantation of olfactory ensheathing cells fails to promote significant axonal regeneration from dorsal roots into the rat cervical cord. J Neurocytol 32:53–70.

Hertel M, Tretter Y, Alzheimer C, Werner S. 2000. Connective tissue growth factor: a novel player in tissue reorganization after brain injury? Eur J Neurosci 12:376–380.

Huang D, Rutkowski JL, Brodeur GM, Chou PM, Kwiatkowski JL, Babbo A, Cohn SL. 2000. Schwann cell-conditioned medium inhibits angiogenesis. Cancer Res 60:5966–5971.

Imaizumi T, Lankford KL, Waxman SG, Greer CA, Kocsis JD. 1998. Transplanted olfactory ensheathing cells remyelinate and enhance axonal conduction in the demyelinated dorsal columns of the rat spinal cord. J Neurosci 18:6176–6185.

Imaizumi T, Lankford KL, Burton WV, Fodor WL, Kocsis JD. 2000. Xenotransplantation of transgenic pig olfactory ensheathing cells promotes axonal regeneration in rat spinal cord. Nat Biotechnol 18:949–953.

Kato T, Honmou O, Uede T, Hashi K, Kocsis JD. 2000. Transplantation of human olfactory ensheathing cells elicits remyelination of demyelinated rat spinal cord. Glia 30:209–218.

Lakatos A, Franklin RJ, Barnett SC. 2000. Olfactory ensheathing cells and Schwann cells differ in their in vitro interactions with astrocytes. Glia 32:214–225.

Lakatos A, Barnett SC, Franklin RJ. 2003. Olfactory ensheathing cells induce less host astrocyte response and chondroitin sulphate proteoglycan expression than Schwann cells following transplantation into adult CNS white matter. Exp Neurol 184:237–246.

Li Y, Field PM, Raisman G. 1997. Repair of adult rat corticospinal tract by transplants of olfactory ensheathing cells. Science 277:2000–2002.

Li Y, Carlstedt T, Berthold CH, Raisman G. 2004. Interaction of transplanted olfactory-ensheathing cells and host astrocytic processes provides a bridge for axons to regenerate across the dorsal root entry zone. Exp Neurol 188:300–308.

Lu J, Feron F, Ho SM, Mackay-Sim A, Waite PM. 2001. Transplantation of nasal olfactory tissue promotes partial recovery in paraplegic adult rats. Brain Res 889:344–357.

McCarthy KD, De Vellis J. 1980. Preparation of separate astroglial and oligodendroglial cell cultures from rat cerebral tissue. J Cell Bio 85:890–902.

Muir EM, Adcock KH, Morgenstern DA, Clayton R, von Stillfried N, Rhodes K, Ellis C, Fawcett JW, Rogers JH. 2002. Matrix metalloproteases and their inhibitors are produced by overlapping populations of activated astrocytes. Brain Res Mol Brain Res 100:103–117.

Nan B, Getchell ML, Partin JV, Getchell TV. 2001. Leukemia inhibitory factor, interleukin-6, and their receptors are expressed transiently in the olfactory mucosa after target ablation. J Comp Neurol 435:60–77.

Navarro X, Valero A, Gudino G, Fores J, Rodriguez FJ, Verdu E, Pascual R, Cuadras J, Nieto-Sampedro M. 1999. Ensheathing glia transplants promote dorsal root regeneration and spinal reflex restitution after multiple lumbar rhizotomy. Ann Neurol 45:207–215.

Pixley SK. 1992. The olfactory nerve contains two populations of glia, identified both in vivo and in vitro. Glia 5:269–284.

Radtke C, Akiyama Y, Brokaw J, Lankford KL, Wewetzer K, Fodor WL, Kocsis JD. 2004. Remyelination of the nonhuman primate spinal cord by transplantation of H-transferase transgenic adult pig olfactory ensheathing cells. FASEB J 18:335–337.

Rajeevan MS, Vernon SD, Taysavang N, Unger ER. 2001. Validation of array-based gene expression profiles by real-time (kinetic) RT-PCR. J Mol Diagn 3:26–31.

Ramer LM, Richter MW, Roskams AJ, Tetzlaff W, Ramer MS. 2004. Peripherally-derived olfactory ensheathing cells do not promote primary afferent regeneration following dorsal root injury. Glia 47:189–206.

Ramon-Cueto A, Nieto-Sampedro M. 1994. Regeneration into the spinal cord of transected dorsal root axons is promoted by ensheathing glia transplants. Exp Neurol 127:232–244.

Ramon-Cueto A, Plant GW, Avila J, Bunge MB. 1998. Long-distance axonal regeneration in the transected adult rat spinal cord is promoted by olfactory ensheathing glia transplants. J Neurosci 18:3803–3815.

Ramon-Cueto A, Cordero MI, Santos-Benito FF, Avila J. 2000. Functional recovery of paraplegic rats and motor axon regeneration in their spinal cords by olfactory ensheathing glia. Neuron 25:425–435.

Richter M, Au E, Liu J, Kwon B, Tetzlaff W, Roskams AJ. 2003. Neoangiogenesis in an ensheathing cell matrix: a trinity of mechanisms to promote spinal cord regeneration. Washington, DC: Society for Neuroscience: Abstract Viewer/Itinerary Planner.

Riddell JS, Enriquez-Denton M, Toft A, Fairless R, Barnett SC. 2004. Olfactory ensheathing cell grafts have minimal influence on regeneration at the dorsal root entry zone following rhizotomy. Glia 47:150–167.

Rozen S, Skaletsky HJ. 2000. Primer3 on the WWW for general users and for biologist programmers. In: Krawetz Stephen A, Misener Stephen, editors. Bioinformatics methods and protocols: methods in molecular biology. Totowa, NJ: Humana Press. p 365–386.

Schwab JM, Beschorner R, Nguyen TD, Meyermann R, Schluesener HJ. 2001. Differential cellular accumulation of connective tissue

growth factor defines a subset of reactive astrocytes, invading fibroblasts, and endothelial cells following central nervous system injury in rats and humans. J Neurotrauma 18:377–388.
Smith PM, Sim FJ, Barnett SC, Franklin RJ. 2001. SCIP/Oct-6, Krox-20, and desert hedgehog mRNA expression during CNS remyelination by transplanted olfactory ensheathing cells. Glia 36:342–53.
Surveyor GA, Brigstock DR. 1999. Immunohistochemical localization of connective tissue growth factor (CTGF) in the mouse embryo between days 7.5 and 14.5 of gestation. Growth Factors 17:115–124.
Takagaki K, Katsuma S, Horio T, Kaminishi Y, Hada Y, Tanaka T, Ohgi T, Yano J. 2003. cDNA microarray analysis of altered gene expression in Ara-C-treated leukemia cells. Biochem Biophys Res Commun 309:351–358.
Takami T, Oudega M, Bates ML, Wood PM, Kleitman N, Bunge MB. 2002. Schwann cell but not olfactory ensheathing glia transplants improve hindlimb locomotor performance in the moderately contused adult rat thoracic spinal cord. J Neurosci 22:6670–6681.
Toews AD, Barrett C, Morell P. 1998. Monocyte chemoattractant protein 1 is responsible for macrophage recruitment following injury to sciatic nerve. J Neurosci Res 53:260–267.
Tran PB, Miller RJ. 2003. Chemokine receptors: signposts to brain development and disease. Nat Rev Neurosci 4:444–455.
Tsukatani T, Fillmore HL, Hamilton HR, Holbrook EH, Costanzo RM. 2003. Matrix metalloproteinase expression in the olfactory epithelium. NeuroReport 14:1135–1140.
Van Den Pol AN, Santarelli JG. 2003. Olfactory ensheathing cells: time lapse imaging of cellular interactions, axonal support, rapid morphological shifts, and mitosis. J Comp Neurol 458:175–194.
Van Der Voorn P, Tekstra J, Beelen RH, Tensen CP, Van Der Valk P, De Groot CJ. 1999. Expression of MCP-1 by reactive astrocytes in demyelinating multiple sclerosis lesions. Am J Pathol 154:45–51.
van Ginkel FW, McGhee JR, Watt JM, Campos-Torres A, Parish LA, Briles DE. 2003. Pneumococcal carriage results in ganglioside-mediated olfactory tissue infection. Proc Natl Acad Sci USA 100:14363–14367.
Vincent AJ, West AK, Chuah MI. 2003. Morphological plasticity of olfactory ensheathing cells is regulated by cAMP and endothelin-1. Glia 41:393–403.
Wewetzer K, Verdu E, Angelov DN, Navarro X. 2002. Olfactory ensheathing glia and Schwann cells: two of a kind? Cell Tissue Res 309:337–345.
Woodhall E, West AK, Chuah MI. 2001. Cultured olfactory ensheathing cells express nerve growth factor, brain- derived neurotrophic factor, glia cell line-derived neurotrophic factor and their receptors. Brain Res Mol Brain Res 88:203–213.
Woodhall E, West AK, Vickers JC, Chuah MI. 2003. Olfactory ensheathing cell phenotype following implantation in the lesioned spinal cord. Cell Mol Life Sci 60:2241–2253.